COMPUTATIONAL EFFICIENCY OF THE FINITE ELEMENT METHOD BASED ON THE SECOND-ORDER RADIATIVE TRANSFER EQUATION

J.M. Zhao[*], J.Y. Tan[**] and L.H. Liu[*+]
[*]Harbin Institute of Technology, 92 West Dazhi Street,
Harbin 150001, People's Republic of China
[**]Harbin Institute of Technology at Weihai, 2 West Wenhua Road
Weihai 264209, People's Republic of China

ABSTRACT. The second-order radiative transfer equation (SORTE) [Numerical Heat Transfer B, Vol. 51, pp. 391-409, 2007] is in a form like diffusion equation, hence no additional artificial diffusion or upwinding treatment is needed in the numerical discretization for stabilization. The computational efficiency of the finite element method based on SORTE is investigated by comparison with that of the finite element methods based on original first order radiative transfer equation (FORTE). The FORTE based finite element methods considered are the finite element method with Galerkin approach (Galerkin-FORTE) and the finite element method with least-square approach (LS-FORTE). By comparison, the accuracy of the finite element method based on the SORTE is generally better than those based on the FORTE under the same discretization scheme, spatial grid and angular grid. The finite element method based on the SORTE shows the best computational efficiency among the three finite element methods, i.e., to obtain the same target accuracy, the least computational time is required.

NOMENCLATURE

$\mathbf{H}$ = Matrix defined in Eq. (10)

$\mathbf{i}, \mathbf{j}, \mathbf{k}$ = Unit vectors of x, y and z direction

$I, \mathbf{I}$ = Radiative intensity, unknown vector of radiative intensity

$\mathbf{K}$ = Stiffness matrix defined in Eq. (10)

L = Side length of enclosure

$\mathbf{n}$ = Unit outward normal vector

N_{sol}, N_{el} = Total number of solution nodes; total number of elements

p = Order of polynomial approximation

q = Radiative heat flux, W/m^2

$\mathbf{r}$ = Spatial coordinates vector

S = Source function defined in Eq. (3)

T = Temperature, K

V = Solution domain

x, y, z = Cartesian coordinates

[*] This work is partly supported by the National Nature Science Foundation of China (50425619, 50906017) and the Development Program for Outstanding Young Teachers in Harbin Institute of Technology (HITQNJS.2009.020), which are gratefully acknowledged.

[+] Corresponding author. *E-mail*: lhliu@hit.edu.cn (L. H. Liu).

β = Extinction coefficient

ε_w = Wall emissivity

ϕ = Shape function

Γ_N = Outflow boundary

Φ = Scattering phase function

κ_a = Absorption coefficient, m^{-1}

κ_s = Scattering coefficient, m^{-1}

μ, ξ, η = Cartesian components of $\mathbf{\Omega}$

σ = Stefan-Boltzmann constant, W/m^2K^4

τ_L = Optical thickness

ω = Scattering albedo

$\mathbf{\Omega}, \mathbf{\Omega}'$ = Vector of radiation direction

Ω = Solid angle

Subscripts

b = Black body

g = Medium

i, j = Spatial solution node index

w = Value at wall

Superscripts

m, m' = The mth discrete ordinate direction

INTRODUCTION

Numerical solution of the radiative transfer in an absorbing, emitting, and scattering medium is of practical importance in many scientific and engineering disciplines. The well known radiative transfer equation (FORTE) is a first order differential equation, which can be written as

$$\mathbf{\Omega} \bullet \nabla I + \beta I = S \tag{1}$$

where $\mathbf{\Omega} = \mu\mathbf{i} + \eta\mathbf{j} + \xi\mathbf{k}$ is the unit direction vector of radiation; β is the extinction coefficient; S is the source function accounting for the thermal emission of medium and in scattering. It is seen that the first term of the left hand side of Eq. (1) can be seen as a convection term with a convection velocity of $\mathbf{\Omega}$, namely, μ, η and ξ are taken as the velocity in x-, y- and z- directions, respectively. Because the vanishing of diffusion term, the FORTE can be considered as a special kind of convection dominated equation [1]. The presence of convection term may cause nonphysical oscillatory of solutions. This type of instability can occur in many numerical methods including finite difference method and finite element method if no special stability treatment is taken, which is one difficulty in the numerical solution of the FORTE.

The traditional differential equation discretization based methods, such as DOM [2], FVM [3-5] and FEM [6, 7], are often based on the FORTE. Because of the convection dominated characteristics of the FORTE, numerical solution of it has to be taken carefully and special stabilization technique is

often necessary for the numerical discretization schemes to correctly model the transfer process. Special stabilization techniques such as upwinding scheme or artificial viscosity are often used in FVM, DOM and FEM. Besides taking various numerical stabilization schemes, another method to overcome the stability problem is to analytically transform the FORTE into a numerically more stable equation, for example, the second order partial differential equation. It is well known that the second order derivative term have the characteristic of diffusion and good numerical properties. The second-order derivative term can serve as a viscosity term to ensure stability of solution, thus additional artificial diffusion or upwinding treatment is not required in the numerical discretization for stabilization. One famous transformed equation is the even-parity formulation (EPF) of the FORTE, which is a second order partial differential equation of the even parity of radiative intensity. Cheong and Song [8] examined several spatial discretization schemes in the discrete ordinates solution of the EPF. Fiveland and Jessee [9, 10] studied the finite element solution of the EPF. Though the stability of the finite element solution of the second order even-parity equation is ensured, numerical results indicate that the solution obtained using the FEM is less accurate as the optical thickness and the wall emissivity are increased.

Recently, a new second-order form of the radiative transfer equation (SORTE) is proposed by Zhao and Liu [11]. The working variable in the SORTE is radiative intensity which is in contrast to the EPF [12] and thus overcomes most of the drawbacks of the EPF. Hassanzadeh and Raithby [13] and Tan et al. [14] evaluated the performance of the SORTE by using the FVM and meshless method. It was demonstrated that the FVM and meshless method based on SORTE can significantly improve the accuracy of solutions. Because of the stability issue caused by the convection term in the FORTE, it is estimated that the requirement of grid number for solving the FORTE should be higher than that for solving the SORTE to obtain the same target accuracy. Hence the computational efficiency of the methods based on FORTE should be lower than that of the SORTE. A comprehensive investigation of the computational efficiency of the SORTE is needed for a broader application of the SORTE. The point is initially demonstrated in Ref. [14] by using meshless method. However, because of the difference of algorithms implemented in different kind of methods, it should be further clarified for FEM implementation.

In this paper, the computational efficiency of the finite element method based on SORTE is investigated by comparison with that of the finite element methods based on FORTE. The FORTE based finite element methods considered are the Galerkin finite element method (Galerkin-FORTE) and the least-squares finite element method (LS-FORTE).

MATHEMATICAL FORMULATION

The discrete-ordinates form of the FORTE [Eq.(1)] in two-dimension can be written as [15]

$$\mu^m \frac{\partial I^m}{\partial x} + \eta^m \frac{\partial I^m}{\partial y} + \beta I^m = S^m, \quad m = 1, 2, \cdots, M \tag{2}$$

where

$$S^m = \kappa_a I_b + \frac{\kappa_s}{4\pi} \sum_{m'=1}^{M} I^{m'} \Phi^{m',m} \, w^{m'} \tag{3}$$

For the opaque and diffuse boundary, the boundary conditions are given as

$$I_w^m = \varepsilon_w I_{bw} + \frac{1-\varepsilon_w}{\pi} \sum_{\mathbf{n}_w \bullet \mathbf{\Omega}^{m'} > 0} I_w^{m'} \left| \mathbf{n}_w \bullet \mathbf{\Omega}^{m'} \right| w^{m'}, \ \ \mathbf{\Omega}^m \bullet \mathbf{n}_w < 0 \tag{4}$$

where $\mathbf{n}_w$ is the unit outward normal vector of the wall; $\mathbf{\Omega}^m = \mu^m \mathbf{i} + \eta^m \mathbf{j}$ is the two-dimensional direction vector; ε_w is the wall emissivity, and $w^{m'}$ is the weight of direction $\mathbf{\Omega}^{m'}$ for angular quadrature.

The presence of the convection terms may cause oscillatory behavior of solutions sometimes. By transforming the original FORTE into a second order equation, the SORTE is formulated into a special diffusion equation, and which can successfully eliminate this kind of nonphysical oscillation [11]. The discrete-ordinates form of the SORTE for homogeneous medium in two-dimension can be expressed as [11]

$$(\mu^m)^2 \frac{\partial^2 I^m}{\partial x^2} + (\eta^m)^2 \frac{\partial^2 I^m}{\partial y^2} + 2\mu^m \eta^m \frac{\partial^2 I^m}{\partial x \partial y} - \beta^2 I^m = U^m \tag{5}$$

where U^m is defined as

$$U^m = \mathbf{\Omega}^m \bullet \nabla S^m - \beta S^m \tag{6}$$

In order to obtain a solution from SORTE, both the inflow boundary and the outflow boundaries are needed to impose boundary conditions. The boundary condition for the inflow boundary ($\mathbf{\Omega}^m \bullet \mathbf{n}_w < 0$) is same as Eq. (4). For the outflow boundary, the boundary condition is given by

$$\mu^m \frac{\partial I^m}{\partial x} + \eta^m \frac{\partial I^m}{\partial y} + \beta I^m = S^m, \ \mathbf{n}_w \bullet \mathbf{\Omega}^m \geq 0 \tag{7}$$

Finite element discretization of the SORTE

In finite element methods, such as traditional finite element method which uses monomial basis or nodal spectral element method which uses orthogonal polynomial as basis, the unknown field variables can be generally approximated by shape functions. For spectral element methods or higher order finite element methods, two kinds of refinement scheme are available to approach the exact result, namely, the traditional mesh refinement (or *h*-refinement) and by increasing the order of polynomial approximation (or *p*-refinement). Both the two kinds of refinement scheme are considered in this paper. Based on the shape function, the radiative intensity of each discrete direction can be approximated as

$$I^m(\mathbf{r}) \simeq \sum_{i=1}^{N_{sol}} I_i^m \phi_i(\mathbf{r}) \tag{8}$$

where ϕ_i is the nodal basis function, I_i^m denotes radiative intensity of direction $\mathbf{\Omega}^m$ at solution nodes i, and N_{sol} is the total number of solution nodes. In this paper, the Chebyshev polynomial expansion is employed to build the shape function on each element. Details on building global nodal basis function were described elsewhere in Ref. [16].

By Galerkin approach, namely, substitute Eq. (8) into the SORTE [Eq.(5)] and do weighted integration by $\phi_j(\mathbf{r})$ over the spatial solution domain yields

$$\sum_{i=1}^{N_{sol}} I_i^m \int_V \left[(\mu^m)^2 \frac{\partial^2 I^m}{\partial x^2} + (\eta^m)^2 \frac{\partial^2 I^m}{\partial y^2} + 2\mu^m \eta^m \frac{\partial^2 I^m}{\partial x \partial y} - \beta^2 I^m \right] \phi_j(\mathbf{r}) \mathrm{d}V = \int_V U^m(\mathbf{r}) \ \phi_j(\mathbf{r}) \mathrm{d}V \tag{9}$$

Following the manipulations presented in Ref. [11], the discretized system of linear equations are obtained as

$$\mathbf{K}^m \mathbf{I}^m = \mathbf{H}^m \tag{10}$$

where

$$K_{ji}^m = \int_V \left[\left(\mu^m \frac{\partial \phi_i}{\partial x} + \eta^m \frac{\partial \phi_i}{\partial y} \right) \left(\mu^m \frac{\partial \phi_j}{\partial x} + \eta^m \frac{\partial \phi_j}{\partial y} \right) + \beta^2 \phi_i \phi_j \right] \mathrm{d}V + \beta \mathbf{\Omega}^m \bullet \int_{\Gamma_N} \phi_i \phi_j \mathbf{n}_w \, \mathrm{d}A \tag{11}$$

$$H_j^m = -\int_V U^m \phi_j \mathrm{d}V + \mathbf{\Omega}^m \bullet \int_{\Gamma_N} S^m \phi_j \mathbf{n}_w \, \mathrm{d}A \tag{12}$$

The source term function S^m can also be expressed using basis function interpolation as

$$S^m(\mathbf{r}) = \sum_{i=1}^{N} S_i^m \phi_i(\mathbf{r}) \tag{13}$$

The stiffness matrices $\mathbf{K}^m$ and $\mathbf{H}^m$ can then be calculated by some tool matrices as

$$\begin{aligned} \mathbf{K}^m = & (\mu^m)^2 \mathbf{A}^{xx} + \mu^m \eta^m \mathbf{A}^{xy} + \eta^m \mu^m (\mathbf{A}^{xy})^T \\ & + (\eta^m)^2 \mathbf{A}^{yy} + \beta^2 \mathbf{B}^{oo} + \beta\left(\mu^m \mathbf{N}^x + \eta^m \mathbf{N}^y\right) \end{aligned} \tag{14}$$

$$\mathbf{H}^m = \left[\beta \mathbf{B}^{oo} - \mu^m (\mathbf{B}^{xo})^T - \eta^m (\mathbf{B}^{yo})^T + \beta\left(\mu^m \mathbf{N}^x + \eta^m \mathbf{N}^y\right)\right] \mathbf{S}^m \tag{15}$$

in which the series of tool matrices $\mathbf{A}$, $\mathbf{B}$ and $\mathbf{N}$ are defined as

$$A_{ji}^{xx} = \int_V \frac{\partial \phi_j}{\partial x}\frac{\partial \phi_i}{\partial x} \mathrm{d}V,\ A_{ji}^{xy} = \int_V \frac{\partial \phi_j}{\partial x}\frac{\partial \phi_i}{\partial y} \mathrm{d}V,\ A_{jn}^{yy} = \int_V \frac{\partial \phi_j}{\partial y}\frac{\partial \phi_i}{\partial y} \mathrm{d}V \tag{16}$$

$$B_{ji}^{xo} = \int_V \frac{\partial \phi_j}{\partial x} \phi_i \,\mathrm{d}V,\ B_{jn}^{yo} = \int_V \frac{\partial \phi_j}{\partial y} \phi_i \,\mathrm{d}V,\ B_{jn}^{oo} = \int_V \phi_j \phi_i \,\mathrm{d}V \tag{17}$$

$$N_{ji}^x = \int_{\Gamma_N} \phi_j \phi_i \,(\mathbf{n}_w \bullet \mathbf{i}) \mathrm{d}A,\ N_{ji}^y = \int_{\Gamma_N} \phi_j \phi_i \,(\mathbf{n}_w \bullet \mathbf{j}) \mathrm{d}A \tag{18}$$

It can be seen that the series of tool matrices, namely, $\mathbf{A}$, $\mathbf{B}$ and $\mathbf{N}$ are independent of angular direction. They only depend on the various integrations of shape functions over the solution domain and the boundary. This indicates that they only need to be calculated and assembled once for all global iteration. The program implementation of the method has best utilized this property to efficiently solve the SORTE, which will be described in following section.

Finite element discretization of the FORTE

Two kinds of finite element discretization are considered for solving the FORTE, namely the Galerkin approach and the least-squares (LS) approach. For Galerkin approach, substitute Eq. (8) into the FORTE [Eq.(2)] and do weighted integration by $\phi_j(\mathbf{r})$ over the spatial solution domain yields

$$\sum_{i=1}^{N_{sol}} I_i^m \int_V \left(\mu^m \frac{\partial \phi_i}{\partial x} + \eta^m \frac{\partial \phi_i}{\partial y} + \beta \phi_i\right) \phi_j \mathrm{d}V = \int_V S^m \,\phi_j \mathrm{d}V \tag{19}$$

The discretized system of linear equations can be written in the form same as Eq. (10), while the stiffness matrices $\mathbf{K}^m$ and $\mathbf{H}^m$ can be calculated by the tool matrices defined above as

$$\mathbf{K}^m = \mu^m (\mathbf{B}^{xo})^T + \eta^m (\mathbf{B}^{yo})^T + \beta \mathbf{B}^{oo} \tag{20}$$

$$\mathbf{H}^m = \mathbf{B}^{oo} \mathbf{S}^m \tag{21}$$

For the LS approach, though it is generally derived from functional minimization, it can also be formulated in a similar way to the Galerkin approach, the different is that the weight function is taken as $\mu^m \frac{\partial \phi_j}{\partial x} + \eta^m \frac{\partial \phi_j}{\partial y} + \beta \phi_j$. The discretized system of linear equations for the LS approach can also be written in the form same as Eq. (10). The stiffness matrices $\mathbf{K}^m$ and $\mathbf{H}^m$ for the LS approach are calculated by the tool matrices defined above as

$$\begin{aligned} \mathbf{K}^m = & (\mu^m)^2 \mathbf{A}^{xx} + \mu^m \eta^m \mathbf{A}^{xy} + \mu^m \beta \mathbf{B}^{xo} \\ & + \eta^m \mu^m (\mathbf{A}^{xy})^T + (\eta^m)^2 \mathbf{A}^{yy} + \eta^m \beta \mathbf{B}^{yo} \\ & + \beta \mu^m (\mathbf{B}^{xo})^T + \beta \eta^m (\mathbf{B}^{yo})^T + (\beta)^2 \mathbf{B}^{oo} \end{aligned} \tag{22}$$

$$\mathbf{H}^m = \left(\mu^m \mathbf{B}^{xo} + \eta^m \mathbf{B}^{yo} + \xi^m \mathbf{B}^{zo} + \beta \mathbf{B}^{oo}\right) \mathbf{S}^m \tag{23}$$

Details on the derivation of LS finite element method for solving the FORTE refer to Ref. [16].

Implementation

For solving the SORTE by the Galerkin finite element approach (Galerkin-SORTE) given above, the outflow boundary condition have been imposed implicitly in the Galerkin discretization formulation by using Gauss theorem, here we use collocation technique to impose the inflow boundary condition, that's, for each node j on the inflow boundary of direction $\mathbf{\Omega}^m$ described by Eq. (4), the stiffness matrix $\mathbf{K}^m$ and right hand side vector $\mathbf{H}^m$ is modified according to

$$K_{ji}^m = \begin{cases} 1, & j = i \\ 0, & j \neq i \end{cases} \tag{24}$$

$$H_j^m = I_j^m \tag{25}$$

For solving the FORTE, the inflow boundary condition is also imposed by the same collocation technique described above for both the Galerkin approach (Galerkin-FORTE) and the LS approach (LS-FORTE).

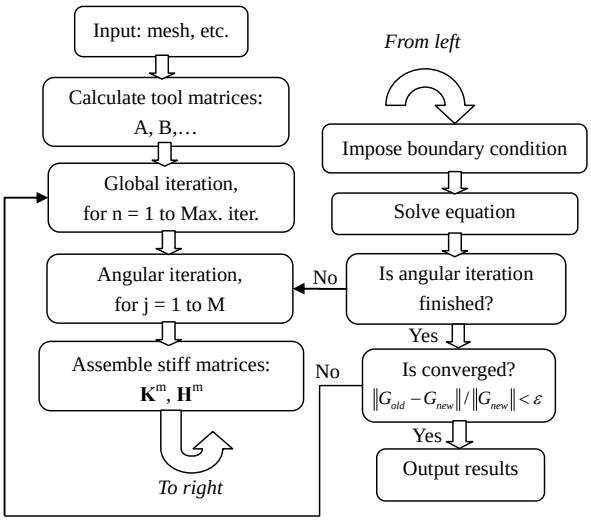

Fig. 1 Generic solution procedures for the finite element methods.

As presented in this paper, the three finite element methods are formulated in a similar manner, thus program code with similar solution procedure can be implemented. A generic solution procedure suitable for all the three finite element methods is carried out according to steps presented in Fig. 1. The major difference in the solution procedure for the three different methods is the assembling of stiffness matrices $\mathbf{K}^m$ and $\mathbf{H}^m$ from tool matrices. The maximum relative error 10^{-4} of incident radiation is taken as stopping criterion for the global iteration.

RESULTS AND DISCUSSION

Computer codes of the three methods, namely, the Galerkin-SORTE, the Galerkin-FORTE and the LS-FORTE are developed based on the formulations and procedures described above. Two distinct test cases are taken to comparatively investigate the accuracy and solution cost of the three methods. As for quantitative evaluation the accuracy of numerical results to the exact results, the maximum relative error is used:

$$\text{Maximum Relative Error \%} = \max\left(\left|\frac{\text{Numerial} - \text{Exact}}{\text{Exact}}\right|\right) \times 100\,, \tag{26}$$

In the following analysis, the computational time is obtained by run the codes on a personal computer with an Intel Core 2 Duo T7100 Processor.

Case 1: Semicircular enclosure with a circular hole

We consider radiative heat transfer in a semicircular enclosure with a circular hole filled with nonscattering gray media as shown in Fig. 2. In this case, the circular hole plays a role as an obstacle. The shielding effect of the obstacle will cause discontinuity in angular distribution of radiative intensity along the bottom wall, which will induce ray effects [17]. The optical thickness of the media is $\tau_L = \beta R$ =0.1. The media is kept hot (T_g =1000K), while all other walls are black and kept cold (0K).

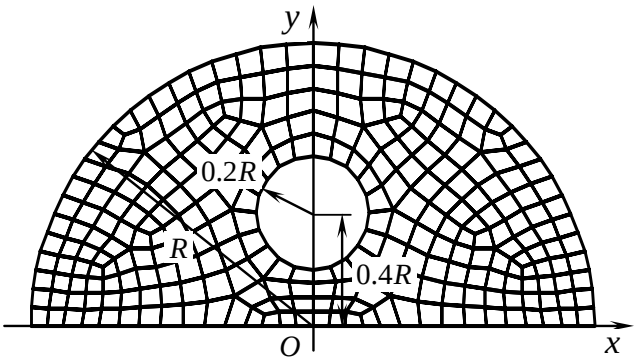

Fig. 2 Configuration of the semicircular enclosure and mesh decomposition (272 elements).

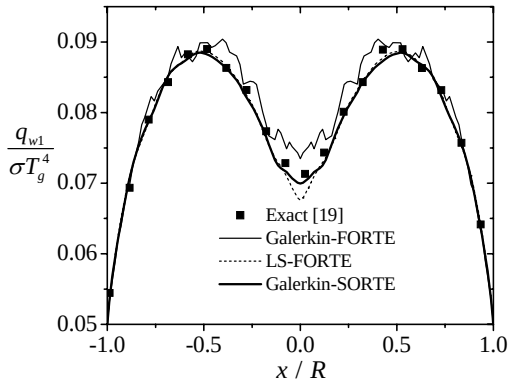

Fig. 3 Dimensionless net radiative heat fluxes distribution on the bottom wall of the semicircular enclosure.

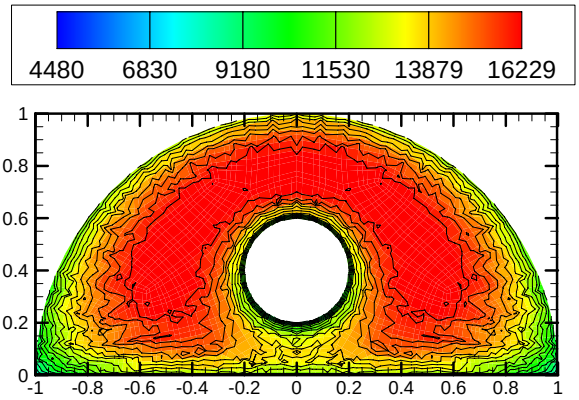

(a) Galerkin-FORTE

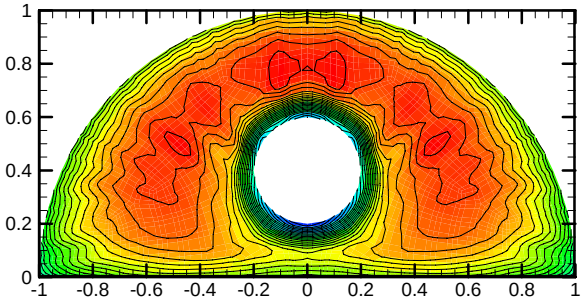

(b) LS-FORTE

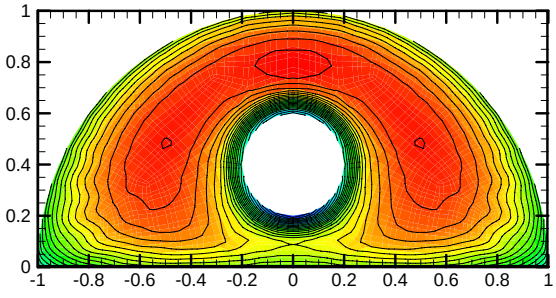

(c) Galerkin-SORTE

Fig. 4 Incident radiation field solved using different finite element approaches based on the FORTE and SORTE.

The three finite element methods based on the FORTE and the SORTE, namely, the Galerkin-SORTE, the Galerkin-FORTE and the LS-FORTE, are all applied to obtain the dimensionless radiative heat flux along the bottom wall ($q_{w1} / \sigma T_g^4$) of the enclosure. The enclosure is decomposed

into 272 quadrilateral elements as shown in Fig. 2. The element shape function is constructed through 3rd order Chebyshev approximation [16]. The angular space is discretized using PCA approach [18] with $N_\theta \times N_\varphi = 20 \times 40$. The solved dimensionless radiative heat flux along the bottom wall is presented in Fig. 3. The exact solution obtained by Kim et al. [19] is taken here as a benchmark. For the finite element methods based on the FORTE, strong unrealistic 'wiggles' are observed in the results obtained by the Galerkin approach, namely, the Galerkin-FORTE. A clearer demonstration is given by the incident field distribution in the medium as shown in Fig. 4. It is shown that the LS-FORTE is more stable than the Galerkin-FORTE, even though, some weak unrealistic wiggles can be observed in the contour lines of incident radiation. However, the result obtained by the finite element method based on the SORTE using the Galerkin approach, namely, the Galerkin-SORTE, is stable and free of nonphysical 'wiggles'. The maximum relative error of the results obtained by the Galerkin-FORTE, the LS-FORTE, and the Galerkin-SORTE, are 4.7%, 5.6% and 2.8%, respectively, which indicate that the Galerkin-SORTE is the most accurate. Though more stable than the Galerkin-FORTE, the LS-FORTE results in a larger relative error than the Galerkin-FORTE, which is explained by its accuracy deteriorate near x=0 as seen in Fig. 3. The Galerkin-SORTE is shown to be the most stable and accurate.

Case 2: Isotropic Scattering Medium in a Square Enclosure

In this case, a square enclosure filled with purely isotropic scattering medium is considered. The bottom wall of the enclosure is kept hot, but all other walls and the medium enclosed by the enclosure are kept cold. The three finite element methods based on the FORTE and the SORTE are applied to this case. The square enclosure is uniformly decomposed into $N_{el} = M \times M$ quadrilateral elements, where M is the number of elements per side of the square enclosure. In this notation, the total number of elements is $N_{el} = M \times M$ and total number of solution nodes is $N_{sol} = \left(M \times p + 1\right)^2$. In the following analysis, the order of polynomial for build nodal shape function is taken as p=1 and the angular space is discretized using S_8 approximation.

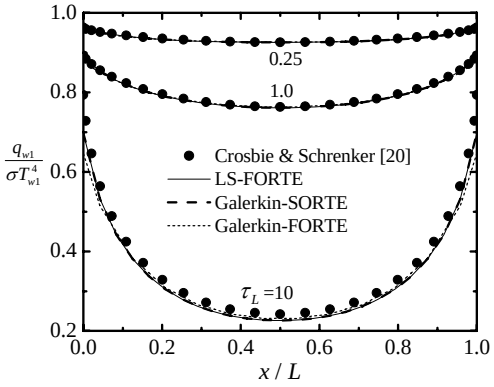

Fig. 5 Dimensionless net radiative heat fluxes distribution on the bottom wall of the square enclosure.

Figure 5 presents the obtained dimensionless heat flux along the bottom wall ($q_{w1} / \sigma T_{w1}^4$) for three values of optical thickness, namely, τ_L=0.25, 1 and 10, by the three finite element methods with $N_{el} = 24 \times 24$ quadrilateral elements. The results obtained by Crosbie and Schrenker [20] is also shown as benchmarks. As for the finite element methods based on the FORTE, the LS-FORTE show better accuracy at high optical thickness (τ_L=10) than the Galerkin-FORTE. Some weak 'wiggles' can also be observed in the results obtained by the Galerkin-FORTE at high optical thickness, which is due to the stability problem related to the Galerkin approach for the FORTE as demonstrated in Case1. The results obtained by the Galerkin-SORTE and the LS-FORTE are

smooth and nearly the same. Detailed analysis of the performance of the three methods is given in the following figures.

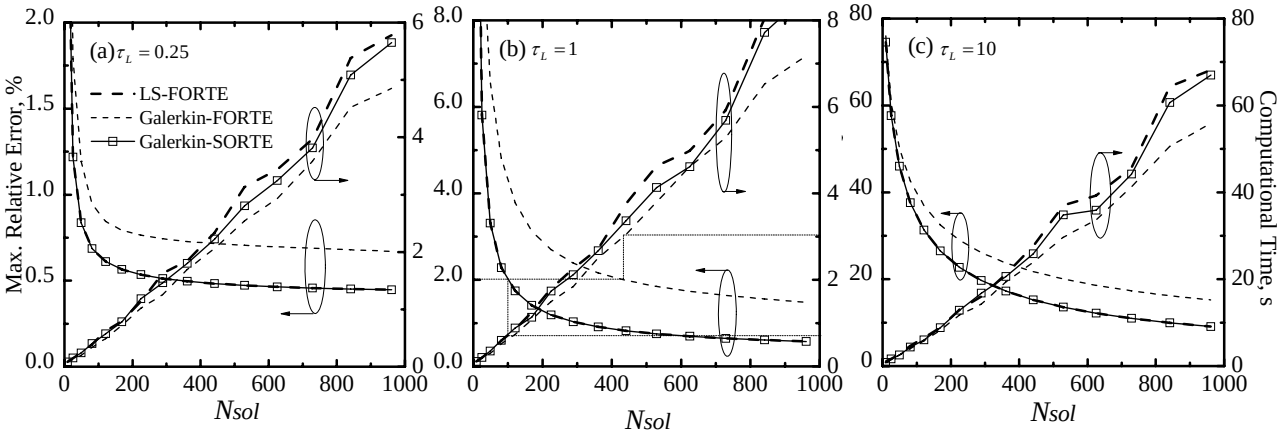

Fig. 6 The convergence characteristics of the finite element methods for different optical thickness.

The convergence characteristics of the three finite element methods are presented in Fig. 6(a)-(c) for three values of optical thickness, namely, τ_L=0.25, 1 and 10, respectively. Generally, under the same spatial decomposition, the accuracy of the Galerkin-SORTE and the LS-FORTE is better than the Galerkin-FORTE, though they tend to require more computational time than the latter. However, to obtain the same accuracy 0.2% as shown in Fig. 6(b), the Galerkin-FORTE requires about 3s, while the Galerkin-SORTE and the LS-FORTE both requires about 0.7s. This indicates that the Galerkin-SORTE and the LS-FORTE has better computational efficiency than the Galerkin-FORTE. The convergence curve of the Galerkin-SORTE and the LS-FORTE is almost the same for different optical thickness; however, the Galerkin-SORTE requires less computational time than the LS-FORTE, which is due to the fact that less computational work is needed in obtain the stiffness matrix $\mathbf{K}^m$ for the Galerkin-SORTE, as can be seen by comparing Eq. (14) and Eq. (22). For different optical thickness, the trends of the curve of convergence and computational time are nearly the same for the finite element methods based on the FORTE and the SORTE. With the optical thickness increasing 10 times (from τ_L=1 to τ_L=10), the accuracy of all the three finite element methods decreases about 10 times, meanwhile, the corresponding computational time increases about 10 times. This reveals that the computational effort is very sensitive to the optical thickness, and is approximately proportional to the square of optical thickness for this case.

CONCLUSION

The computational efficiency of the finite element method based on SORTE is investigated by comparison with that of the finite element methods based on FORTE. The LS-FORTE gives comparable stability and accuracy with the Galerkin-SORTE under same computational conditions, while the computational time of the Galerkin-SORTE is shorter than that of the LS-FORTE, especially for strong scattering medium. The stability and accuracy of the Galerkin-SORTE and the LS-FORTE is better than the Galerkin-FORTE, though they tend to require more computational time than the latter. However, to obtain the same accuracy, much more computational time is needed for the Galerkin-FORTE, which illustrates that the Galerkin-SORTE and the LS-FORTE has better computational efficiency than the Galerkin-FORTE. By comparison, the accuracy of the finite element method based on the SORTE is generally better than those based on the FORTE under the same discretization scheme, spatial grid and angular grid. The finite element method based on the SORTE shows the best computational efficiency among the three finite element methods.

REFERENCES

1. Chai, J. C., Lee, H. S. and Patankar, S. V., Finite-Volume Method for Radiation Heat Transfer, In:W. J. Minkowycz and E. M. Sparrow (eds.), *Advances in Numerical Heat Transfer*, Taylor & Francis, New York, pp. 109-141, 2000.
2. Fiveland, W. A., Three-Dimensional Radiative Heat-Transfer Solutions by the Discrete-Ordinates Method, *J. Thermophys. Heat Transfer*, Vol. 2, pp 309-316, 1988.
3. Raithby, G. D. and Chui, E. H., A Finite-Volume Method for Predicting a Radiant Heat Transfer in Enclosures with Participating Media, *ASME J. Heat Transfer*, Vol. 112, pp 415-423, 1990.
4. Chai, J. C. and Lee, H. S., Finite-Volume Method for Radiation Heat Transfer, *J. Thermophys. Heat Transfer*, Vol. 8, pp 419-425, 1994.
5. Murthy, J. Y. and Mathur, S. R., Finite Volume Method for Radiative Heat Transfer Using Unstructured Meshes, *J. Thermophys. Heat Transfer*, Vol. 12, pp 313-321, 1998.
6. Kisslelev, V. B., Roberti, L. and Perona, G., An Application of the Finite-Element Method to the Solution of the Radiative Transfer Equation, *J. Quant. Spectrosc. Radiat. Transfer*, Vol. 51, pp 603-614, 1994.
7. Liu, L. H., Finite Element Simulation of Radiative Heat Transfer in Absorbing and Scattering Media, *J. Thermophys. Heat Transfer*, Vol. 18, pp 555-557, 2004.
8. Cheong, K. B. and Song, T. H., Examination of Solution Methods for the Second-Order Discrete Ordinate Formulation, *Numer. Heat Transfer B*, Vol. 27, pp 155-173, 1995.
9. Fiveland, W. A. and Jessee, J. P., Finite Element Formulation of the Discrete-Ordinates Method for Multidimensional Geometries, *J. Thermophys. Heat Transfer*, Vol. 8, pp 426-433, 1994.
10. Fiveland, W. A. and Jessee, J. P., Comparison of Discrete Ordinates Formulations for Radiative Heat Transfer in Multidimensional Geometries, *J. Thermophys. Heat Transfer*, Vol. 9, pp 47-54, 1995.
11. Zhao, J. M. and Liu, L. H., Second Order Radiative Transfer Equation and Its Properties of Numerical Solution Using Finite Element Method, *Numer. Heat Transfer B*, Vol. 51, pp 391-409, 2007.
12. Lewis, E. E. and Miller, W. F., *Computational Methods of Neutron Transport*, Wiley, New York 1984.
13. Hassanzadeh, P. and Raithby, G. D., Finite-Volume Solution of the Second-Order Radiative Transfer Equation: Accuracy and Solution Cost, *Numerical Heat Transfer Part B-Fundmental*, Vol. 53, pp 374-382, 2008.
14. Tan, J. Y., Zhao, J. M., Liu, L. H. and Wang, Y. Y., Comparative Study on Accuracy and Solution Cost of the First/Second-Order Radiative Transfer Equations Using the Meshless Method, *Numerical Heat Transfer, Part B: Fundamentals*, Vol. 55, pp 324 - 337, 2009.
15. Modest, M. F., *Radiative Heat Transfer*, 2nd ed, Academic Press, San Diego, 2003.
16. Zhao, J. M. and Liu, L. H., Least-Squares Spectral Element Method for Radiative Heat Transfer in Semitransparent Media, *Numer. Heat Transfer B*, Vol. 50, pp 473-489, 2006.
17. Zhao, J. M. and Liu, L. H., Discontinuous Spectral Element Method for Solving Radiative Heat Transfer in Multidimensional Semitransparent Media, *J. Quant. Spectrosc. Radiat. Transfer*, Vol. 107, pp 1-16, 2007.
18. Liu, L. H., Zhang, L. and Tan, H. P., Finite Element Method for Radiation Heat Transfer in Multi-Dimensional Graded Index Medium, *J. Quant. Spectrosc. Radiat. Transfer*, Vol. 97, pp 436-445, 2006.
19. Kim, M. Y., Baek, S. W. and Park, J. H., Unstructured Finite-Volume Method for Radiative Heat Transfer in a Complex Two-Dimensional Geometry with Obstacles, *Numer. Heat Transfer B*, Vol. 39, pp 617-635, 2001.
20. Crosbie, A. L. and Schrenker, R. G., Radiative Transfer in a Two-Dimensional Rectangular Medium Exposed to Diffuse Radiation, *J. Quant. Spectrosc. Radiat. Transfer*, Vol. 31, pp 339-372, 1984.